Understanding Sampling Error Characteristics in Ensemble-based Estimates of Land-atmosphere Coupled Background Error Covariances in a Dryline CI case study

Aaron Johnson and Xuguang Wang
University of Oklahoma School of Meteorology
Consortium for Advanced Data assimilation Research and Education (CADRE)
Acknowledgement: Clara Draper, Michael Barlage, Terra Ladwig

Introduction

- A strongly coupled approach to DA (SCDA) that uses all available observations to provide consistent analyses across the land-atmosphere interface poses significant practical challenges (e.g., Penny et al. 2017; de Rosnay et al. 2022).
- It has been shown that ensemble-based SCDA of screen level atmosphere observations to update soil moisture state variables can lead to mesoscale model forecast improvements over the central U.S. (Lin an Pu 2020).
- An important open question related to land-atmosphere SCDA has to do with how sampling errors resulting from the finite ensemble size are treated.

- Distance-based covariance localization is often used to treat sampling error in ensemble-based DA (Houtekamer and Mitchel 1998) but has challenges for SCDA.
  - Sampling error can increase abruptly for nearby variables across the interface between Earth System components (Stanley et al. 2024)
  - The temporal and spatial scales of variability in the different components may be quite different (Stanley et al. 2021)
  - The true correlation between cross-component variables may be smaller than within-component correlations (e.g., Smith et al. 2017)
- The optimal treatment of sampling error during ensemble-based land-atmosphere SCDA likely depends on the characteristics of the coupled correlations and their sampling error which are not well known at convective- and meso-scales.

- Dryline convection initiation (CI) is sensitive to characteristics of the land surface (e.g., Trier et al. 2004; Martin and Xue 2006; Duda et al. 2017).
- Therefore, a dryline CI event provides a good starting point to begin to investigate ensemble-based estimation of land-atmosphere coupled error correlations and their potential applicability for SCDA in regional convection-allowing data assimilation and forecast systems.

- In particular, the goal of this case study is to provide insight into the physical relationships between soil and atmosphere variables on the time and space scales relevant to dryline CI prediction, and guide future efforts to treat sampling error in ensemble-based land-atmosphere SCDA in convection-allowing regional models.

Case Overview

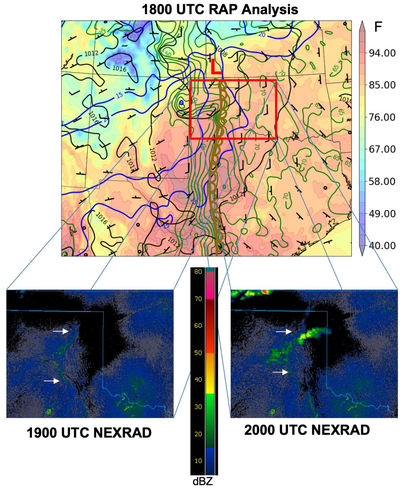

Fig 1: 1800 UTC 19 May 2024 operational RAP analysis of (shading) 2m T, (green contours) 2m Td at 5 Fahrenheit interval starting at 30 F, (black contours) MSLP at 4 hPa interval, and (blue) 500 hPa wind speed at 5 m/s interval starting at 15 m/s. Lower panels show NEXRAD composite reflectivity in the indicated region at (left) 1900 and (right) 2000 UTC. White arrows highlight location of radar fine line associated with observed dryline.

- Weak synoptic scale forcing and pressure minimum in southwest KS associated with moderate intensity (~25 m/s maximum) 500 hPa jet streak.
- Dryline extends southward through eastern TX panhandle.
- 10m flow southerly ahead of dryline, southwesterly behind it.
- CI occurs in northeast TX panhandles between 1900 and 2000 UTC

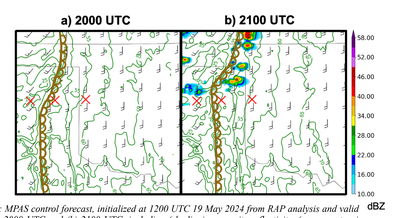

Fig 2: MPAS control forecast, initialized at 1200 UTC 19 May 2024 from RAP analysis and valid at (a) 2000 UTC and (b) 2100 UTC, including (shading) composite reflectivity, (green contour) 2m Td and (barbs) 10 m wind in knots. Approximate dryline location is shown in standard symbol, and red crosses are locations of hypothetical observations used in section 3.

- Mesoscale environment, including 2m dewpoint gradient associated with dryline, is well simulated (Fig. 2).
- CI occurs in similar location as observed, about 1 hour later than observed.
- Study focuses primarily on the 2000 UTC time, just before CI.
- Locations of three hypothetical observations used later are indicated by red crosses in Fig 2a.

Experiment Design

- Ensemble forecasts using CONUS-domain, 3km grid spacing MPAS (GSL-dev version 8.2.2), initialized from RAP analysis with soil state perturbations
- 4-day cycling period is used to spin up realistic ensemble diversity in the soil state variables directly on the 3km grid (Fig. 3).
- 8-hour free forecast ensemble from 1200 UTC spins up the coupled ensemble perturbations as planetary boundary layer (PBL) develops during the day
- Similar coupled correlations could be expected to develop during a 6-8hr cycling period in regional cycled DA
- Ensemble dressing (Wang and Bishop 2005) to generate 1000-member ensemble of SMOIS, TSLB, T, QVAPOR from the resulting 30-member ensemble

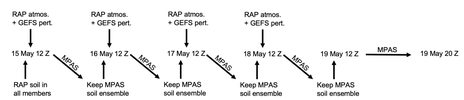

Fig 3: Diagram of 4-day cycling period used to spin up soil state ensemble

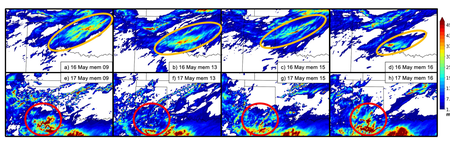

Fig. 4: 24-hour precipitation accumulation for representative members during spin-up period for the forecasts ending at (top row) 1200 UTC 16 May and (bottom row) 1200 UTC 17 May precipitation. Features emphasized in the text are highlighted with orange and red circles.

- Precipitation during spin up period is expected to dominate soil moisture variability.
- The first two days of the spin up period were particularly convectively active in this region (Fig. 4).
- During first day, variability in track and intensity of upscale growing SW-to-NE propagating MCS (top row; orange circles).
- During second day, variability in how much precipitation occurred in NW TX (bottom row; red circles)

1000-member Ensemble Correlations

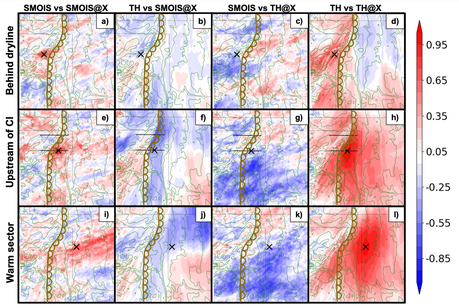

Fig 5: 1000-member ensemble correlation between (first column) 4cm soil moisture (i.e., SMOIS) and a hypothetical observation of SMOIS, (second column) model level 5 Potential temperature (i.e., TH) and a hypothetical observation of SMOIS, (third column) SMOIS and a hypothetical observation of TH and (fourth column) TH and a hypothetical observation of TH. The hypothetical observation location is indicated by the "x" (top row) behind the dryline, (middle row) directly upstream of CI and (bottom row) in the warm sector. Green contours are as in Fig. 2a for reference.

- Hypothetical TH5 observation is strongly correlated to TH5 in surrounding mesoscale area, especially east of dryline (Fig. 5; 4th column)
- Hypothetical SMOIS observation is correlated to SMOIS at larger distances, with more elongated shape, as observation moves from west to east (1st column)
  - Corresponds to upscale growing MCS variability during spin up period.
- SMOIS observation contains more information about TH5 downstream from the observation (e.g., in the region of CI; panel f) than at the observation.
- Similarly, TH5 observations are most strongly correlated to SMOIS well upstream of the TH5 observation (3rd column)

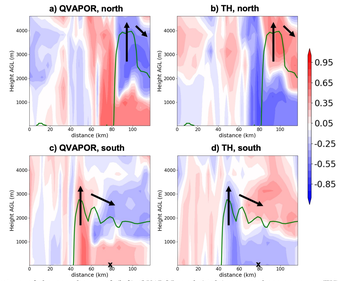

Fig 6: Cross sections of the correlation of (left) QVAPOR and (right) potential temperature (TH) to the hypothetical observation of 4cm soil moisture located upstream of CI. The location of the cross sections is shown on Figure 5. The correlations in (top) northern cross section and (bottom) southern cross section are both with respect to the location of a hypothetical observation in the plane of the southern cross section and marked with an "x". Dark green contour of ensemble mean 4 g/kg of QVAPOR indicates the approximate boundary of the moist warm sector boundary layer for reference. Arrows indicate approximate location of vertical moisture lofting and compensating subsidence in ensemble mean forecast.

- Hypothetical SMOIS observation ("x" in Fig. 6c,d, Fig 5e-h) is positively correlated to moisture in the lower boundary layer and along/west of the vertically lofted moisture (Fig. 6a,c)
  - Negatively correlated with moisture in the upper PBL and subsiding branch of dryline circulation (Fig. 6a,c)
  - Potential temperature correlations have similar structure, opposite sign (Fig. 6b,d)
- Correlations are qualitatively similar along the downstream cross-section, but with greater magnitude, even several km above the surface (Fig. 6a,b)
- Strongest correlations in southern cross section are within rising branch of the dryline circulation (Fig. 6c,d; suggesting intensity).
- Strongest correlations in northern cross section are just west of the vertical moisture lofting in the ensemble mean (Fig. 6a,b; suggesting location)

Horizontal Distribution of Sampling Error

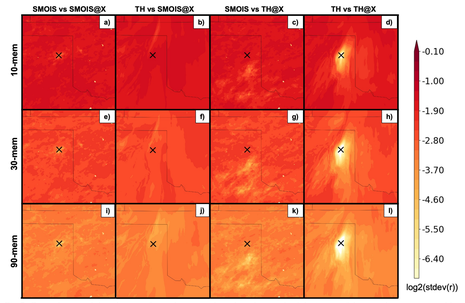

Fig 7: Example spatial distribution of sampling error based on the standard deviation of the correlation estimated by resampled sub-ensembles of (top row) 10, (middle row) 30, and (bottom row) 90 ensemble members. The correlations used to quantify sampling error are the correlation of (first column) SMOIS to a hypothetical SMOIS observation at the "x", (second column) TH5 to a hypothetical SMOIS observation at the "x", (third column) SMOIS to a hypothetical TH5 observation at the "x", and (fourth column) TH5 to a hypothetical TH5 observation at the "x"

- Sub-ensembles of different sizes are repeatedly sampled to quantify sampling error by the standard deviation of sub-ensemble correlations
- Smallest sampling errors (Fig. 7) generally correspond to largest correlations (Fig. 5)
- Sampling error decrease from 30 to 90 members raises question of what ensemble size is needed
- Smallest sampling error at observation location for auto-correlations (1st and 4th columns), spatially displaced for cross-correlations (2nd and 3rd columns)
- Treatment of sampling error that assumes it to increase with distance from the observation should not be expected to perform well for SCDA of this case.

- For autocorrelations, (Fig. 8bc) the true correlation (black lines) decreases with distance while sampling error increases (Fig. 8c) or remains similar (Fig. 8c)
- For TH5 autocorrelation (Fig. 8c), the decrease of true correlation occurs over a larger spatial scale than for the SMOIS autocorrelation (Fig 8b).
- Average cross-correlation magnitude is less than 0.5, decreasing to less than 0.25 beyond ~20-30km (Fig. 8a,d)
- Sampling error for cross-correlations is in general larger than for auto-correlations.
- As distance from the observation increases, the sampling error either remains similar (Fig. 8a) or decreases (Fig. 8d).

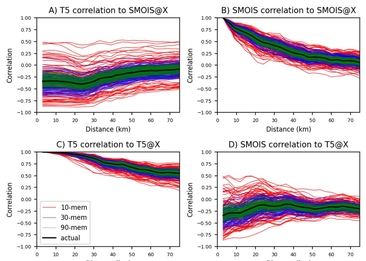

Fig 8: Correlation as a function of distance for the hypothetical observation located upstream of CI, based on (a) TH5 correlation to a hypothetical SMOIS observation, (b) SMOIS correlation to a hypothetical SMOIS observation, (c) TH5 correlation to a hypothetical TH5 observation, and (d) SMOIS correlation to a hypothetical TH5 observation. Black lines show the actual correlation in the 1000-member ensemble, averaged over all grid points at each distance from the observation with a bin width of 3 km. Red, blue and green lines are for randomly selected sub-ensembles of 10-, 30- and 90-members, respectively.

- TH5 autocorrelation sign is reliably estimated with ~10 members east of the dryline, ~100 members west of the dryline, within 70km distance (Fig. 9c).
- SMOIS autocorrelation sign is reliably estimated with < 100 members within 50km of the "upstream of CI" observation (Fig. 9b black line)
  - Generally requires 100s of members at the other locations.
- Cross-component correlations are also estimated most reliably at the "upstream of CI" location (Fig. 9a,d black lines).
  - Highlights dryline CI as a region of locally enhanced land-atmosphere coupling
- All correlations are generally more challenging to estimate west of the dryline (blue lines).

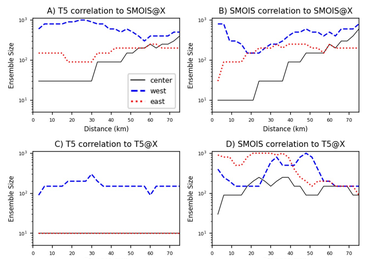

Fig 9: Smallest ensemble size at which 2 times the average sampling error, calculated as the standard deviation of correlation based on randomly sampled ensemble members, is less than the absolute value of the actual correlation on average at the same distance from the hypothetical observation. The calculation is repeated for the same hypothetical observations as in Fig. 7, which were (black solid) centrally located upstream from CI, (blue dashed) shifted west in the dry air mass, and (red dotted) shifted east into the warm sector airmass.

Vertical Distribution of Sampling Error

Fig 10: (top row) correlation between 4cm soil moisture and (a) water vapor or soil moisture at different levels above or below ground, respectively, and (b) potential temperature or soil temperature at different levels above or below ground, respectively, for the center hypothetical observation, located upstream of CI in Fig. 5, in the (black) 1000-member ensemble, (red) 10-member ensembles, (blue) 30-member ensembles and (green) 90-member ensembles. (bottom row) Ensemble size needed to reliably estimate sign of correlation, calculated as in figure 9, for all three locations of hypothetical observations. The approximate top of the boundary layer is indicated by a horizontal line at the first level where ensemble mean potential temperature increases with height.

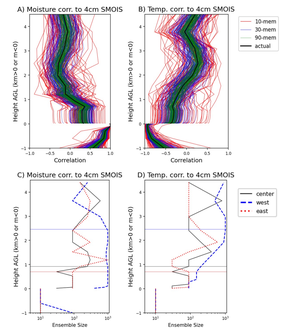

- At the upstream of CI location, SMOIS observation is most strongly correlated to soil state in the top 0.5 m (Fig. 10a,b).
- Magnitudes of correlation to low level water vapor and potential temperature are less than ~0.5 (Fig. 10a,b).
- Sampling error of correlation to the atmosphere variables is qualitatively similar as height increases (Fig. 10a,b).

- At all three locations, sign of correlation to other soil variables is reliably estimated with 10 members (Fig. 10c.d).
- Larger ensembles needed above PBL
  - Especially at "center"/"east" locations in moist airmass (Fig. 10c,d; red and black lines).
- West of dryline, SMOIS observation contains little reliable information about the atmosphere variables (Fig. 10; c,d blue lines)

Fig 11. As in figure 10, except for a model level 5 potential temperature hypothetical observation.

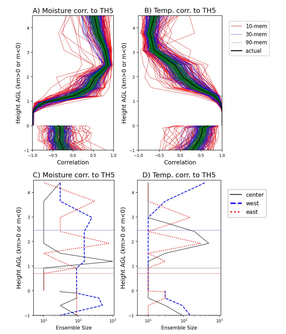

- TH5 observation is most strongly correlated to other variables in the lowest ~1km of the atmosphere (Fig. 11a,b).
- Magnitude of actual correlation is relatively small, and the qualitative spread of sampling error is relatively large, at ~1.5-2.5km (Fig. 11a,b)
  - i.e., Sampling error is not monotonically decreasing with height even when only considering the atmosphere variables.
- Magnitude of correlation to soil state variables is roughly 0.25-0.5, with qualitatively large sampling error (Fig. 11a,b)

- TH5 observation correlation to temperature is reliably estimated with 10 members within PBL (Fig. 11d)
  - Maximum in sampling error just above the boundary layer.
- Correlation to water vapor reliably estimated in PBL with 10 members only east of the dryline (Fig. 11c; black and red lines).
- Correlation to top ~0.5 m of soil variables is estimated reliably at smaller ensemble sizes for the upstream of CI locations than the other locations (Fig. 11c,d; black lines)
  - Further suggests locally increased importance of land-atmosphere coupling for DA in the vicinity of dryline CI.

Fig 12. As in figure 10 (center observation location only), except that the column of atmosphere variables is shifted 30km north (i.e., downstream) from the hypothetical observation and column of soil variables

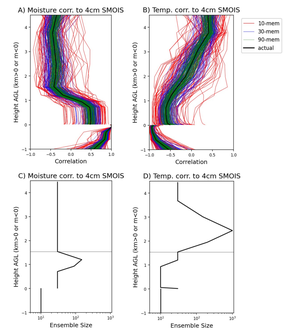

- Upstream of CI SMOIS observation has stronger correlations to atmosphere variables at the downstream location near CI than for the atmospheric column directly above the hypothetical observation (Fig. 11a,b).
- Sign of correlation to downstream water vapor is reliably estimated with 30 members (Fig. 11c)
  - Exception is upper PBL where up to 100-200 members are needed.
- Sign of correlation to downstream potential temperature also reliably estimated with 10-30 ensemble members at many height levels (Fig. 11d)
  - Exception is the layer just above the boundary layer at ~2-3km AGL.

Summary and Future Work

- A case of dryline CI is used to explore the land-atmosphere coupled correlation structure and its sampling error.
- Eigenvectors of 30-member MPAS ensemble forecast with soil state initial condition perturbations, and coupled soil-atmosphere perturbations by the 8-hour forecast time, are used to generate a 1000-member ensemble from which sub-ensembles are drawn to quantify sampling error.

- Autocorrelations within soil and atmosphere variables have different spatial scales, which also depend on location of hypothetical observation.
- Cross-correlations between soil and atmosphere variables (i.e., land-atmosphere coupling) are particularly strong just east of the dryline, upstream of CI.
- Hypothetical soil moisture observation contains information about the strength and location of dryline and its associated circulation.

- Cross-correlations have greatest magnitude, and least sampling error, at a location spatially displaced from the observation itself.
- Vertical extent of correlation to soil moisture observation is related to PBL depth, with large sampling error near top of PBL.

- Convective-scale land-atmosphere ensemble-based SCDA may benefit from treating sampling error differently for autocorrelations and cross-correlations.
- Flow-dependent and anisotropic nature of sampling error should also be accounted for in the SCDA

References

- Duda J. D., X. Wang, M. Xue, 2017: Sensitivity of convection-allowing forecasts to land surface model perturbations and implications for ensemble design. *Mon Weather Rev*, **145**, 2001–2025.
- Houtekamer, P. L., H. L. Mitchell, 1998. Data assimilation using an ensemble Kalman filter technique. *Mon. Weather Rev,* **126,** 796–811.
- Lin, L.-F., and Z. Pu, 2020: Improving near-surface short-range weather forecasts using strongly coupled land–atmosphere data assimilation with GSI-EnKF. *Mon. Wea. Rev.*, **148**, 2863–2888
- Martin, W., and M. Xue, 2006: Sensitivity analysis of convection of the 24 May 2002 IHOP case using very large ensembles. *Mon. Wea. Rev.*, ***134***, 192–207
- Penny, S. G., and Coauthors, 2017: Coupled data assimilation for integrated earth system analysis and prediction: Goals, challenges and recommendations. WMO Tech. Rep. WWRP 2017-3, 59 pp
- de Rosnay, P., and coauthors 2022: Coupled data assimilation at ECMWF: Current status, challenges and future developments. *Quarterly Journal of the Royal Meteorological Society*, **148**, 2672–2702
- Smith, P. J., A. S. Lawless, N. K. Nichols, 2017: Estimating forecast error covariances for strongly coupled atmosphere–ocean 4D-Var data assimilation. *Monthly Weather Review*, **145**, 4011–4035
- Stanley, Z., I. Grooms, W. Kleiber, 2021: Multivariate localization functions for strongly coupled data assimilation in the bivariate Lorenz 96 system. *Nonlinear Processes in Geophysics*, **28**, 565–583
- Stanley, Z. C., C. Draper, S. Frolov, L. C. Slivinski, W. Huang, H. R. Winterbottom, 2024: Vertical localization for strongly coupled data assimilation: Experiments in a global coupled atmosphere-ocean model. *Journal of Advances in Modeling Earth Systems*, **16**, e2023MS003783.
- Trier, S. B., F. Chen, and K. W. Manning, 2004: A study of convection initiation in a mesoscale model using high-resolution land surface initial conditions. *Mon. Wea. Rev.*, ***132***, 2954–2976
- Wang, X. and C. H. Bishop, 2005: Improvement of ensemble reliability with a new dressing kernel. *Q. J. R. Meteorol. Soc.*, **131**, 965–986.